Available online at www.sciencedirect.com

ScienceDirect

Energy Procedia 4 (2011) 4347–4353

Energy Procedia

www.elsevier.com/locate/procedia

Two phase brine-CO_2 flow experiments in synthetic and natural media

Jonathan S. Levine[a]*, Juerg M. Matter[b], David S. Goldberg[b], Klaus S. Lackner[a]
Michael G. Supp[c], T.S. Ramakrishnan[c]

[a] *Department of Earth and Environmental Engineering, Columbia University, 500 West 120th St #918, NY, NY 10027*
[b] *Lamont Doherty Earth Observatory, Columbia University, 61 Route 9W, Palisades NY, 10964*
[c] *Schlumberger-Doll Research, 1 Hampshire St, Cambridge, MA 02139*

Abstract

Industrial scale injection of anthropogenic carbon dioxide into the crustal lithosphere has been proposed to reduce atmospheric accumulation. Much of this injection is expected to occur in saline reservoirs. An understanding of two-phase brine-CO_2 flow is necessary for predicting storage capacity, fluid migration, and injectivity in geologic reservoirs. Additionally, the chemical reactivity of the rock matrix with $CO_{2(l)}$ affects the transport properties of the rock. A flow system for measuring two-phase transport of CO_2 and brine is presented in this paper. The system is capable of displacing brine with either liquid or supercritical CO_2. Special effort was taken to circumvent capillary end-effects in these experiments. Drainage end point relative permeability of CO_2 displacing brine is found to be in the range of 0.34-0.44, much lower than what is expected for a nonwetting fluid. Such low relative permeabilities would tend to decrease injectivity while increasing displacement efficiency.

Keywords: CO_2, relative permeability, experiments

1. Introduction

Anthropogenic carbon dioxide emission to the atmosphere is thought to be the primary source of global warming and ocean acidification [1]. Geologic carbon sequestration, the injection of CO_2 emissions into porous rock formations, has been proposed as a possible solution [2]. In addition to suitable proximity, three important criteria are prerequisite for a site: containment, capacity, and injectivity. Injectivity is limited by the geomechanical constraints, and the permeability-thickness product of the reservoir. To determine both pressure rise and fluid migration requires multi-phase reservoir-scale modeling. Currently, the models and simulation relating to CO_2 displacement assume in large part that the process is similar to gas displacement of water. Given the practical implications of injectivity, laboratory scale experiments are necessary to confirm or alter what has been the conventional practice although clearly they do not consider the complicating factors seen at the field scale.

We present a set of relative permeability experiments for CO_2 displacing water in both natural and artificial cores. The experiment is designed in such a way as to obtain only the relative permeability of CO_2 displacing water at residual water saturation – the so called "drainage" relative permeability. Although the entire curve may be defined, we have at this juncture focused on quantifying the end-point mobility of CO_2 at residual water. While this state only corresponds to conditions sufficiently behind the saturation transition zone, it has enormous implication with regard to the shape of the plume as has been discussed in other publications.

* Corresponding author. Tel: 617-768-2151
Email address: jsl183@columbia.edu

doi:10.1016/j.egypro.2011.02.386

2. Multiphase Flow in Porous Media

Under conditions of minimal reactivity with the rock matrix, the extended form of Darcy's law and local capillary equilibrium describe two-phase flow. These are

$$v_w = -\frac{kk_{rw}}{\mu_w}\nabla p_w \tag{1}$$

$$v_n = -\frac{kk_{rn}}{\mu_n}\nabla p_n \tag{2}$$

$$p_c(S_w) = p_n - p_w \tag{3}$$

with the velocity of the two phases w and n being denoted by v with the appropriate subscripts, the permeability being k, the relative permeabilities shown with a subscript r along with the phase, the viscosity being denoted by μ along with the appropriate subscript, and pressure of the phase i being p_i. The pressure difference between n and w is the capillary pressure, which depends on the saturation. For closure, a continuity equation is needed, so that the saturation and the pressures can be obtained for specific initial and boundary condition (see, e.g., [3]).

Owing to occupancy criteria under conditions of local capillary equilibrium, it is well known that the relative permeability to the nonwetting phase approaches unity when residual wetting phase saturation is approached [4, 5]. For the present systems, it is commonly thought that under supercritical conditions, water would wet the solid in relation to the less-dense state of CO_2. Data reported in the literature point otherwise [6, 7].

In a displacement experiment in which the nonwetting phase displaces the wetting phase, the saturation profile transitions from close to residual wetting phase at the inlet to a sharp capillary transition zone, and then to the connate wetting phase saturation. Additionally, at the outlet of the core, the wetting fluid is retained, and the saturation corresponds to a zero capillary pressure (see [8, 9]). This end-effect plays a significant role in the interpretation of the displacement data and the additional resistance to flow of the nonwetting fluid must be removed in the calculations. The end-effect persists even the displaced fluid is not strongly wetting, except that the outlet may not be fully saturated with this fluid.

The purpose of the experiments here were two-fold. Firstly, it was to develop a system that could operate under a range of temperatures and pressures relevant to sequestration. Secondly, it was also necessary to verify whether the end-point relative permeabilities for CO_2 across a range of natural and synthetic rocks remain low as has been reported elsewhere, even after the end-effect is removed.

3. Materials and Methods

We designed and built a high pressure core flooding reactor at Schlumberger-Doll Research in Cambridge, MA for the purpose of measuring multiphase flow properties. The experimental design is shown in Figure 1. This design pushes liquid or supercritical CO_2 (0 °C–90 ºC, up to 100 bar) through a brine-saturated core sample at a series of constant flow rates while the pressure drop across the core is monitored. These are done at a fixed outlet pressure, and is monitored and controlled. The same is true of the radial confining stress. A brief description of sample preparations and experimental runs are presented below. The details of the apparatus are contained in [10].

Sample preparation and apparatus

Natural and synthetic cores were used under a variety of conditions using the flow system. Natural cores included Berea sandstone, chosen for its relative homogeneity, and prior experimental data availability, synthetic P3C alumina ceramic (CoorsTek™), which has little sample variability and immeasurable sample reactivity to carbonated water. Helium intrusion porosity measurements were made on 3.8 cm (1.5") diameter, 3.8 cm (1.5") long cores adjacent to the experiment's cores that were 10 cm (4") in length and 3.8 cm (1.5") in diameter. Later experiments were conducted with 20 cm (8") length P3C cores to further reduce end-effects. All cores were vacuum dried overnight at 70 °C prior to each experiment.

During each experiment cores were placed in a high-pressure (up to a flowing pressure of ≈100 bars/1,500 psi) core holder held vertically in a stand that allowed hydraulic and electrical connections. Cores were sealed in a rubber sleeve made of either Viton fitted with a pair of impedance terminals or Buna-N with a jacketing pressure of 135 bars (≈2,000 psi). Radial pressure was applied with an electrically nonconductive fluorinert FC-40 by a syringe pump in

constant pressure mode. A precision impedance analyzer was used to monitor impedance and phase angle. The core holder and pressure transducers were contained in a temperature-controlled chamber with a rated accuracy of 0.3 °C. All tubing and fittings were Swagelok stainless steel 316L and were leak tested to < 10 nL/s with a He leak detector. Prior to each experiment, an oil-free vacuum pump was used to evacuate air from the system for 12-24 hours.

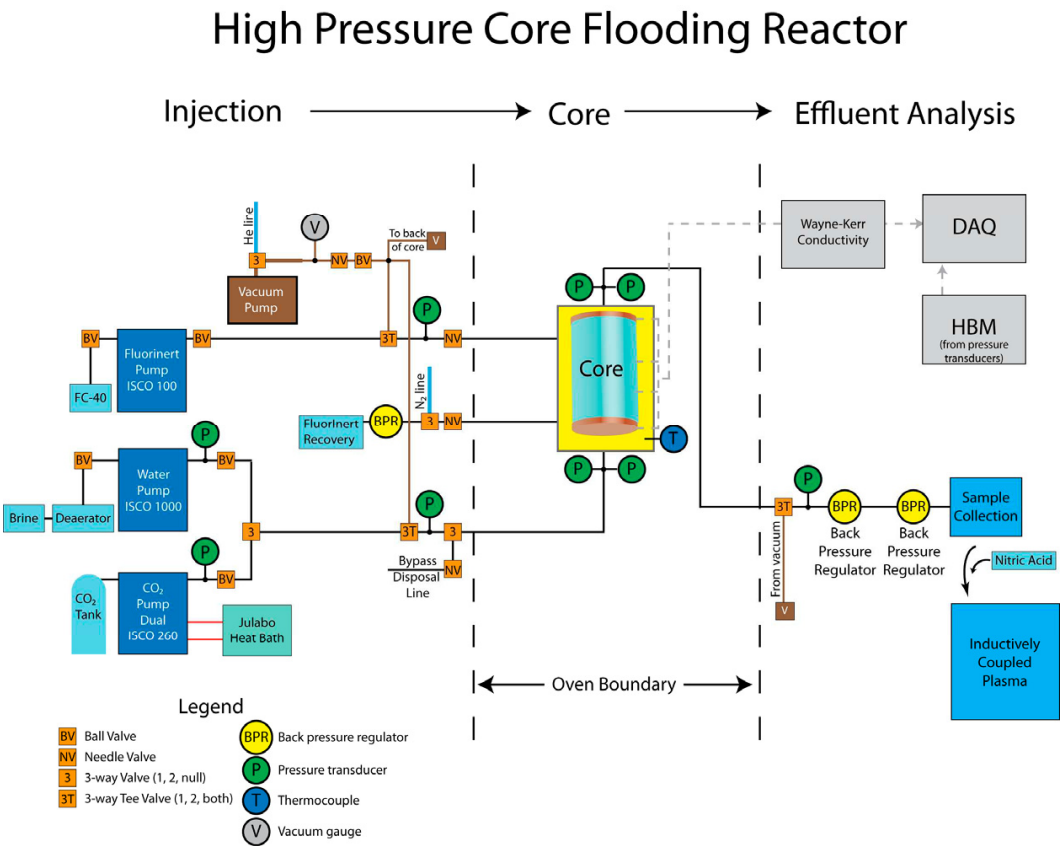

Figure 1: Schematic of the experimental apparatus

Fluid injection and measurement

Samples were initially flooded with an aqueous solution containing 50,000 mg/kg NaCl (ACS Grade) and 50 mg/kg LiCl (ACS Grade) tracer to be used to test for salt precipitation. Later experiments with P3C alumina cores used deionized (DI) water of 18.2 MΩ cm, and confirmed that salt precipitation did not significantly affect permeability measurements. Aqueous solution was loaded from a deaerator directly into an evacuated syringe pump under vacuum. For reference, brine was also sampled via a bypass line immediately before the core flood. All geochemical measurements were made relative to this reference. CO_2 was dispensed at a constant flow rate from a paired set of temperature controlled syringe pumps with an air valve package to minimize pressure transients at pump switchover. Liquid CO_2 was siphoned directly from a CO_2 cylinder (99.8% bone dry). In all cases cores were held vertically. For quality check, initial experiments injected CO_2 into the core from below to align buoyancy and viscous instabilities; later experiments injected CO_2 from above to create a buoyancy-stabilized plume front. System pressure was controlled by two back pressure regulators in series with the first electronically controlled and the second manually set to approximately 5–10 bars less than the experimental pressure, with the first regulator fully opened. Effluent was sent to a sampling system consisting of 20 high-pressure 40 mL sampling containers (stainless steel 304L coated with a 0.001" PTFE) for mass balance measurement of residual water saturation as well as elemental analysis by ICP spectroscopy.

Pressure measurements and instrument calibration

Low-pressure measurements of fluids in the experimental system were made with 10 bar pressure transducers (0.1% full scale accuracy). High-pressure measurements were made with 200 bar pressure transducers (0.2% full scale accuracy). Transducers were connected via seven wire cables to an excitation-measurement processing system with 18-bit accuracy. The seven wire system enabled us to ensure that the excitation voltage did not suffer from line losses. The amplified digital output was passed through a 1.25 Hz Bessel filter. Pressure measurements were collected in chunks of 128 data points, collected almost instantaneously and averaged. Low-pressure transducers were simultaneously calibrated relative to a portable calibrator with 0.025% accuracy. High-pressure transducers were simultaneously calibrated with a primary standard dead weight tester (5 ppm mass accuracy). The pressure offset between transducers located before and after the core was corrected in each experiment by a linear fit between at least a pair of offset measurements. All equipments were monitored by a data acquisition system capable of automatically gathering, processing, and analyzing the data in real time.

Permeability measurements

Brine permeability was measured at atmospheric pressure as well as at experimental fluid pressure (100 bar). Permeability measurements were made by flowing brine with increasing and then decreasing flow rates in evenly spaced increments, (e.g. 0–3 mL/min in 0.5 mL/min increments) while limiting the highest flow rate to maintain a Reynolds number below 0.5 to ensure laminar flow [11]. At least three independent measurements of permeability were made and their average reported for each experiment. Effective radial stress was controlled to be 35 bars in both low- and high- pressure measurements. In several instances post-experiment cores were vacuum oven dried overnight, reloaded, evacuated of air overnight, and then, liquid CO_2 was used to saturate the core sample. High pressure (100 bar) liquid CO_2 permeability was measured, and in all cases, the brine permeability agreed with that of CO_2.

CO_2 *flood experiments*

At the beginning of each experiment, air was evacuated from the core overnight. The core was then saturated with brine and brine permeability obtained at low and high pressures. CO_2 was then used to purge the system of brine up to the core holder via a bypass to minimize CO_2/brine mixing and carbonic acid formation before the core itself. CO_2 pressure was then raised to 100 bar. After about an hour, of stabilization, CO_2 was injected in a series of incremental flow rates, until the pressure drop across the core had stabilized. Flow rates were chosen so that each experiment lasted no longer than 3-4 hours, avoiding any additional salt precipitation induced effects. The first flow rate was chosen based upon on a numerical estimate of breakthrough time by solving a non-linear diffusion operator as discussed in reference [12]. Flow was doubled until a reasonably high flow rate, typically around 10 mL/min, and then increased in linear steps until the system's maximum stable flow rate was achieved at approximately 30–50 mL/min (see Figure 2 below). The maximum CO_2 saturation is reached at the inlet of the core, with a monotonic decrease to a saturation corresponding to $p_c = 0$ at the outlet. Because pore occupancy is controlled by capillarity, the ratio of the pressure drop at a given flow rate to the breakthrough pressure, $\Delta P/P_b$, corresponds to the ratio of the smallest pore throat radius occupied at breakthrough to the smallest pore throat radius at the flow rate of interest. Therefore, a high $\Delta P/P_b$ ratio ensures that the residual water saturation is approached at the inlet. While the pressure drop is sufficiently large to reach residual water at the inlet, the capillary number, the ratio of viscous to capillarity induced pressure drop is kept sufficiently small, below the level needed to mobilize residual water (see [13]). The pressure drop as a function of flow rate reaches a constant slope at the larger rates, and this measurement technique may be used to corrected for capillary end effects as given by [9]:

$$k_{rn}^0 = \frac{\mu_n}{kA}\frac{dQ}{dP_n} \tag{4}$$

This result is different from taking simply the ratio of the flow rate to the pressure drop.

Sources of measurement error

Three sources of error are possible. The first is the evaporation of water, which would increase the mobility to CO_2 by opening up fluid pathways. The second is the precipitation of salt, which might cause a minor reduction in the mobility. Therefore, our conclusions were tested by repeating the same procedure with a synthetic rock in which distilled, deionized water is used rather than a salt solution. Finally, additional experimental error occurred at high pressure because of fluctuations in the back pressure regulator approaching a bar. Experimental data was noisy, varying by 5-10%, but not affecting the overall trends in the data (see [10]).

4. Results

We summarize the results of the Berea sandstone and P3C alumina ceramic displacement experiments. Results from an example experiment are shown in Figures 2 and 3. Experimental conditions are noted in the figure captions.

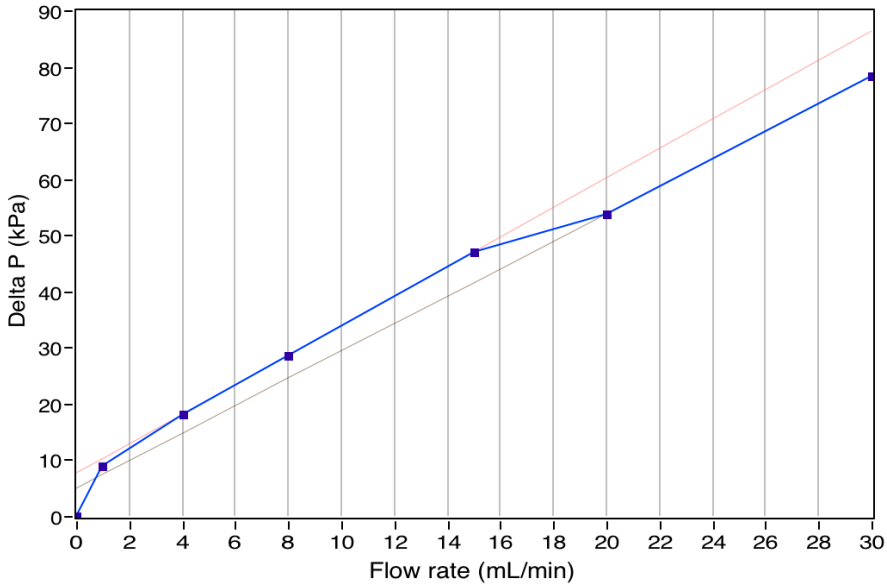

Figure 2: Sample results: Berea 100 sandstone core at 20 °C, 100 bar, 1% NaCl, k_{r_CO2}=0.44
A drop in backpressure between 15 and 20 mL/min caused a subsequent decline in pressure drop, but the data is consistent on either side of this shift with k_{r_CO2}=0.41 between 4 and 15mL/min and k_{r_CO2}=0.44 between 20 and 30 mL/min.

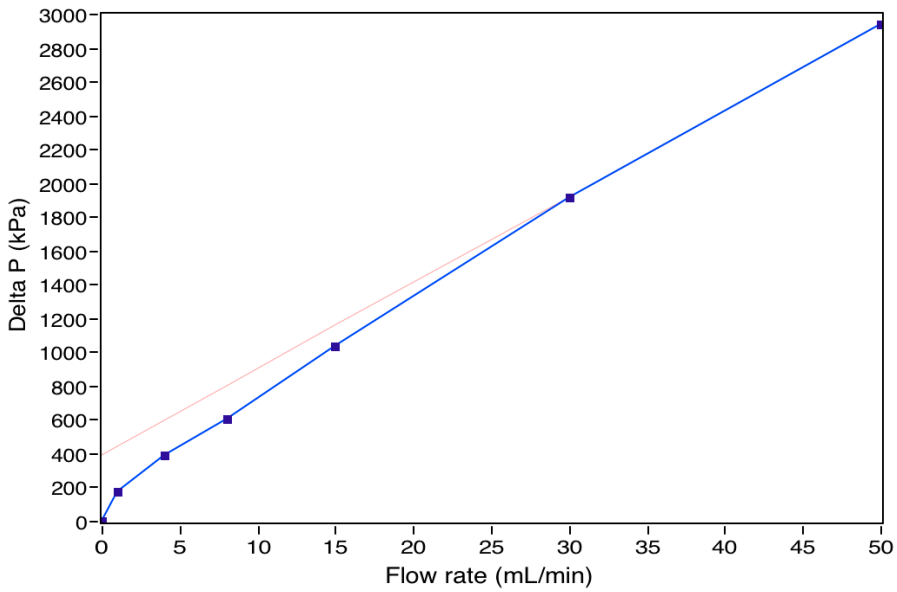

Figure 3: Sample results: P3C alumina ceramic core at 20 °C, 100 bar, DI water, kr_CO2=0.34

A summary of experimental conditions and results for a selected subset of experiments is shown in Table 1. The experiments universally had intermediate values of end point drainage CO2 relative permeability. The first experiments were a P3C alumina ceramic (12.2 mD) and a higher permeability (655 mD) Berea sandstone with a 5% brine at liquid CO2 conditions (100 bar, 20°C). These experiments were repeated with CO2 flooding from the top of the core rather than the bottom followed by testing a lower permeability Berea (120 mD) with a less saline brine (1% NaCl) to reduce any effects due to salt.

Core	Pressure (bars)	Temp (°C)	CO_2 state	Brine	Length (cm)	Permeability (mD)	End point CO_2 relative permeability
Berea 500	100	20	Liquid	5%	10	665	0.38
Berea 100	100	20	Liquid	1%	10	116	0.44
P3C	100	20	Liquid	5%	10	12.0	0.34
P3C	100	20	Liquid	DI	20	12.2	0.34
P3C	100	50	Supercritical	DI	20	12.1	0.37

Table 1: Summary of conditions and results for drainage end point relative permeability of CO_2 displacing water.

Next, experiments were conducted with synthetic inert and homogeneous P3C alumina and with deionized water in place of 5% brine to eliminate any extraneous effects due to salt. We also carried out several experiments at supercritical conditions (100 bar, 50 °C) and far away from both the gas-liquid and liquid-hydrate transitions on the CO_2 phase diagram. Finally a set of experiments was performed with a modified setup at 20°C with varying back pressure including gas and liquid phase CO_2 (10, 20, 35, 65 bars) with similar results. In all cases, we found drainage end point relative permeability values (twelve experiments in total) to be tightly clustered, with seven experiments between 0.34-0.40, an additional three experiments in the range of 0.30-0.50, and two outlier measurements at values of 0.19 and 0.56. This result suggests that conventional assumption of CO_2 having a relative permeability close to unity may be inappropriate.

5. Discussion

Given the common assumption of CO_2 being a nonwetting fluid in relation to aqueous solutions of common salt, we anticipated that the drainage endpoint relative permeability of (inert) CO_2 displacing water would be in the range of 0.8–1. Instead, all of our experiments resulted in intermediate values for relative permeability of CO_2 displacing water, more typical of a weakly wetted system. Other recent investigations of the relative permeability of CO_2 displacing brine have found surprisingly low values [6, 7]. These intermediate values imply that CO_2 cannot be treated as an inert nonwetting phase for mobility calculations. Even a supercritical CO_2 displacement has low values of end-point relative permeability. Experiments with CO_2 in silica aerogels as well as molecular dynamics simulations between CO_2 and muscovite have shown CO_2 layers bound to mineral surfaces [14]. Contact angle measurements of saturated CO_2 and water on quartz and mica show an increasing angle as high as 60° through the water phase with increasing pressure and salinity [15]. Quantitative CO_2-water-mineral contact angle measurements are needed, especially under conditions of storage.

Lower CO_2 relative permeability will affect the flow of CO_2 in reservoirs in several ways. Storage capacities will be decreased in pressure-limited reservoirs where storage capacities are determined by the caprock fracturing pressure. CO_2 migration and the shape of the plume are functions of mobility ratio in dipping beds [16, 17], and therefore fixing this ratio is quite critical for determining capacity. Furthermore, if, as evidenced by the end-point mobility, CO_2-water systems are weakly-wet, counter imbibition of water may be ineffective, thus reducing residual trapping. Therefore, petrophysical analyses for potential CO_2 sequestration sites should include core-scale relative permeability measurements to improve the ability to calculate plume migration more accurately than what is prevalent today.

6. Conclusion

Endpoint relative permeability experiments of CO_2 displacing water from synthetic and natural rock cores at both liquid and supercritical conditions have been performed. Endpoint CO_2 relative permeabilities are shown to have intermediate values with the results tightly clustered around 0.35-0.4. We conclude that CO_2 cannot be treated as an inert nonwetting phase and further pore-scale experiments are needed to explain the underlying reasons for this result. Based on these results, pressure-limited reservoirs will have reduced capacity while area-limited reservoirs will have increased capacity. Finally, because injectivity and storage capacity are highly sensitive to relative permeability, future

petrophysical analyses for potential CO_2 sequestration sites should include relative permeability measurements on reservoir core samples rather than relying on extrapolations based on prior studies.

Acknowledgements

J.L. acknowledges the entire CO_2 research group at Schlumberger-Doll Research for help with experiments as well as fruitful discussions. This work was supported by a NYSERDA grant (NYSERDA-10113) and J.L. acknowledges support from the US National Science Foundation, through a Fellowship in the IGERT Joint Program in Applied Mathematics and Earth and Environmental Science at Columbia University.

References

[1] IPCC, "The physical science basis," Contribution of Working Group I to the Fourth Assessment Report of the Intergovernmental Panel on Climate Change, 2007.
[2] IPCC, *IPCC Special Report on Carbon Dioxide Capture and Storage*. IPCC, 2005.
[3] K. Aziz and A. Settari, *Petroleum Reservoir Simulation*, 1979.
[4] G. Willhite, *Waterflooding*. Society of Petroleum Engineers, Richardson, TX, 1986.
[5] W. Anderson, "Wettability Literature Survey Part 5: The Effects Of Wettability On Relative Permeability," *Journal of Petroleum Technology*, vol. 39, no. 11, pp. 1453–1468, 1987.
[6] S. Bachu and B. Bennion, "Effects of in-situ conditions on relative permeability characteristics of CO2-brine systems," *Environmental Geology*, vol. 54, no. 8, pp. 1707–1722, 2008.
[7] J. Perrin and S. Benson, "An Experimental Study on the Influence of Sub-Core Scale Heterogeneities on CO_2 Distribution in Reservoir Rocks," *Transport in porous media*, vol. 82, no. 1, pp. 93–109, 2010.
[8] J. Douglas Jr., P.M. Blair, and R.J. Wagner, "Calculation of linear waterflood behavior including the effects of capillary pressure", *Petroleum Transactions*, *AIME*, vol. 213, pp. 96-102, 1958.
[9] T.S. Ramakrishnan and A. Cappiello, "A new technique to measure static and dynamic properties of a partially saturated porous medium," *Chemical engineering science*, vol. 46, no. 4, pp. 1157–1163, 1991.
[10] J. Levine, *Relative permeability experiments of carbon dioxide displacing water & their implications for carbon sequestration,* Ph.D. thesis, Columbia University, 2010.
[11] A. Scheidegger, *The physics of flow through porous media*, 1974.
[12] R. Sivakumar and T.S. Ramakrishnan, "Dynamics of Inviscid Wetting Phase Displacement in a Relative Permeability Measurements," internal Schlumberger research report, February 2006.
[13] H. S. Dombrowski and L. E. Brownell, "Residual Equilibrium Saturation of Porous Media", *Industrial &Engineering Chemistry,* vol. 46 no. 6, pp. 1207-1219, 1954.
[14] D.R. Cole, Chialvo, A. A. , Rother, G. , Vlcek, L., and P. T. Cummings, "Supercritical fluid behavior at nanoscale interfaces: Implications for CO2 sequestration in geologic formations" *Philosophical Magazine*, vol. 90, no. 17, pp. 2339–2363, 2010.
[15] P. Chiquet, D. Broseta, and S. Thibeau, "Wettability alteration of caprock minerals by carbon dioxide," *Geofluids*, vol. 7, no. 2, pp. 112–122, 2007.
[16] M. A. Hesse, B.T. Mallison, and H.A. Tchelepi, "Compact Multiscale Finite Volume Method for Heterogeneous Anisotropic Elliptic Equations", *Multiscale Model. Simul.* 7, 934, 2008.
[17] R. de Loubens and T.S. Ramakrishnan, "Analysis and Computation of Gravity Induced Migration in Porous Media", submitted to *J.Fluid Mech.,* 2010.